CORE
Metadata, citation and similar papers at core.ac.uk
Provided by Warwick Research Archives Portal Repository

University of Warwick institutional repository: http://go.warwick.ac.uk/wrap

This paper is made available online in accordance with publisher policies. Please scroll down to view the document itself. Please refer to the repository record for this item and our policy information available from the repository home page for further information.

To see the final version of this paper please visit the publisher's website. Access to the published version may require a subscription.

Author(s): Keith N. Leppard, Edward Emmott, Marc S. Cortese and Tina Rich

Article Title: Adenovirus type 5 E4 Orf3 protein targets promyelocytic leukaemia (PML) protein nuclear domains for disruption via a sequence in PML isoform II that is predicted as a protein interaction site by bioinformatic analysis

Year of publication: 2009
Link to published version:
http://dx.doi.org/ 10.1099/vir.0.005512-0

Publisher statement: This is an author manuscript that has been accepted for publication in Microbiology, copyright Society for General Microbiology, but has not been copy-edited, formatted or proofed. Cite this article as appearing in Microbiology. This version of the manuscript may not be duplicated or reproduced, other than for personal use or within the rule of 'Fair Use of Copyrighted Materials' (section 17, Title 17, US Code), without permission from the copyright owner, Society for General Microbiology. The Society for General Microbiology disclaims any responsibility or liability for errors or omissions in this version of the manuscript or in any version derived from it by any other parties. The final copy-edited, published article, which is the version of record, can be found at http://mic.sgmjournals.org, and is freely available without a subscription.

Adenovirus type 5 E4 Orf3 protein targets PML nuclear domains for disruption via a sequence in promyelocytic leukaemia protein isoform II that is predicted as a protein interaction site by bioinformatic analysis.

Keith N Leppard[1*], Edward Emmott[1a], Marc S Cortese[2] and Tina Rich[2]

[1] Department of Biological Sciences, University of Warwick, Coventry, CV4 7AL, U.K.; [2] Institute of Comparative Medicine, University of Glasgow, Glasgow, G61 1QH, U.K.

Words in main text: 5462

Words in summary: 210

Number of Figures & Tables: 7

Running Title: Adenovirus 5 Orf3 protein binding site on PMLII

[a] Present address: Institute of Molecular and Cellular Biology & Astbury Centre for Structural Molecular Biology, University of Leeds, Leeds, UK, LS2 9NZ

* corresponding author:

Department of Biological Sciences

University of Warwick

Coventry, CV4 7AL, U.K

Phone: +44 24 7652 3579

Fax: +44 24 7652 3701

Email: Keith.Leppard@warwick.ac.uk

26 **Summary**

27 Human adenovirus type 5 infection causes the disruption of structures in the cell
28 nucleus termed PML nuclear domains or ND10, which contain promyelocytic
29 leukaemia protein (PML) as a critical component. This disruption is achieved through
30 the action of the viral E4 Orf3 protein, which forms track-like nuclear structures that
31 associate with PML protein. This association is mediated by a direct interaction of
32 Orf3 with a specific PML isoform, PMLII. We show here that the Orf3 interaction
33 properties of PMLII are conferred by a 40 amino acid residue segment of the unique
34 C-terminal domain of the protein. This segment was sufficient to confer interaction on
35 a heterologous protein. The analysis was informed by prior application of a
36 bioinformatic tool for the prediction of potential protein interaction sites within
37 unstructured protein sequences (PONDR® analysis). This tool predicted three
38 potential molecular recognition elements (MoRE) within the C-terminal domain of
39 PMLII, one of which was found to form the core of the Orf3 interaction site thus
40 demonstrating the utility of this approach. The sequence of the mapped Orf3 binding
41 site on PML was found to be relatively poorly conserved across other species,
42 however the overall organization of MoREs within unstructured sequence was
43 retained, suggesting the potential for conservation of functional interactions.

44 **Introduction**

45 Human adenovirus type 5 (Ad5) is one of a diverse collection of viruses that interact
46 during infection with nuclear structures termed ND10 or PML nuclear domains (PML-
47 NDs (reviewed in Everett & Chelbi-Alix, 2007, Leppard & Dimmock, 2006). These
48 structures are complex multiprotein assemblies within which promyelocytic leukaemia
49 (PML) protein is a key component, essential for the localization of other proteins to
50 PML-NDs. PML-NDs have been implicated in a variety of important cell processes,
51 including DNA damage & stress responses, senescence, apoptosis and innate
52 immunity (Bernardi & Pandolfi, 2007).

53

54 The targeting of PML-NDs by viruses has been linked to avoidance of innate immune
55 responses. The incoming genomes of several nucleus-replicating DNA viruses
56 localize adjacent to PML-NDs (Ishov & Maul, 1996). For herpes simplex virus type 1
57 (HSV1) this has been shown to involve the mobilization of existing PML-ND
58 components to the sites of virus ingress (Everett & Murray, 2005). Both HSV1 and
59 human cytomegalovirus infections induce the gross disruption of PML-NDs and, for
60 HSV1, degradation of PML protein (Everett & Maul, 1994, Kelly et al., 1995). Ad5
61 infection disrupts PML-NDs by deforming them into a large number of elongated
62 tracks (Carvalho et al., 1995, Doucas et al., 1996). For both HSV1 and Ad5,
63 mutations that prevent expression of the virus-coded PML-ND disruption function
64 leave the viruses highly sensitive to innate and intrinsic antiviral responses (Everett
65 et al., 2008, Everett et al., 2006, Ullman & Hearing, 2008, Ullman et al., 2007). Thus
66 it has been proposed that PML-NDs or their components play a key role in the
67 detection of virus infection and/or the subsequent cellular response and that

68 consequently many viruses have evolved proteins that target and modify this PML-

69 ND function.

70

71 The *pml* gene encodes six C-terminally variant nuclear PML protein isoforms (I – VI)

72 that contribute to PML-ND formation and these are further modified by covalent

73 attachment of SUMO proteins to up to three lysine residues within their common N-

74 terminal domain (Fig. 1A) (Borden et al., 1996, Fagioli et al., 1992, Jensen et al.,

75 2001, Sternsdorf et al., 1997). Assembly of PML into PML-NDs requires the N-

76 terminal RBCC motif (Fig1A) (Borden et al., 1996) and is thought to be mediated by

77 non-covalent binding of attached SUMO groups to an interaction motif encoded by

78 exon 7a and present in isoforms I – V (Shen et al., 2006). The gene also encodes

79 several cytoplasmic PML isoforms that lack the the nuclear localization signal

80 because of exon-skipping during mRNA splicing which have unique functions

81 (Salomoni & Bellodi, 2007).

82

83 The Ad5 function that targets PML-NDs is the Orf3 protein, encoded by the E4

84 transcription unit, which draws PML into co-localization with it in characteristic tracks

85 (Carvalho et al., 1995, Doucas et al., 1996). This Orf3 function is conserved among

86 diverse human adenoviruses (Evans & Hearing, 2003), unlike its ability to reorganise

87 the DNA repair complex, MRN, which is specifically a feature of Orf3 from species C

88 human Ads (Stracker et al., 2005). These two activities have been separated

89 genetically. Recently, we showed that Orf3 targets PML-NDs via a specific and direct

90 interaction with nuclear PML isoform II (Hoppe et al., 2006). Mutations in Orf3 that

91 abrogated its ability to bind PMLII also eliminated its ability to rearrange PML-NDs.

92 The aim of the present study was to define the sequences within PMLII that were
93 responsible for binding Orf3. To achieve this, a targeted deletion strategy was
94 employed, informed by both homology comparisons between PMLII proteins from
95 three species and also the application of a predictive bioinformatic tool for identifying
96 potential protein interaction sites within amino acid sequences (PONDR®). From the
97 properties of these mutant proteins, a 40 amino acid segment of the PMLII C-
98 terminus was found to be necessary and sufficient for Orf3 binding. The propensity of
99 this region of PMLII for protein interactions was independently predicted by PONDR®
100 analysis, demonstrating the utility of this approach to the mapping of protein : protein
101 interactions.

102

103 **Methods**

104 *Plasmid cloning and mutagenesis*

105 N-terminally FLAG-tagged PML cDNA clones in pCIneo expressing nuclear isoforms
106 I - VI (Beech et al., 2005), and a Ad5 E4 Orf3 expression plasmid (Hoppe et al.,
107 2006), have been described previously. The PML ΔRBCC deletion links the N-
108 terminal FLAG epitope to PML residue 361, immediately distal to the RBCC motif. It
109 was constructed by single-round PCR using FLAG-PML V template DNA with one
110 primer bridging the FLAG-PML junction and the second complementary to PML exon
111 5; a restriction fragment containing the deletion was then used to replace the
112 equivalent fragment in each of the pCIFLAG-PML cDNA clones. Specific deletions in
113 PMLII ΔRBCC were constructed by a two-stage PCR protocol using two common
114 primers complementary to PML exon 6 and the vector distal to the cDNA insert, and
115 pairs of mutagenic primers designed to fuse the coding sequence in frame at the
116 desired location. Restriction fragments from second round PCR products were

117 substituted for the corresponding wild-type sequence encoding amino acids 555 to
118 the C-terminus within PMLII ΔRBCC. To construct a GFP expression clone tagged
119 with PMLII-derived sequences, plasmid phrGFP-N1 (Stratagene) was first modified to
120 tag the hrGFP C-terminus with the SV40 large T antigen nuclear localization signal,
121 GPKKKRKVG (Kalderon et al., 1984), and designated phrGFP-NLS. The sequence
122 encoding PMLII amino acids 645-684 was amplified by PCR incorporating a BglII site
123 at the N-terminal end and a stop codon plus EcoRI restriction site at the C-terminal
124 end, suitable for cloning in-frame into phrGFP-NLS to generate phrGFP-NLS-m1m2.
125 All clones were verified by DNA sequencing; primer sequences are available on
126 request.
127
128 *Cells and transfection*
129 U2OS human osteosarcoma cells were maintained in McCoy's 5A medium (Gibco)
130 supplemented with 10% fetal bovine serum. Transfections of plasmid DNA were
131 carried out using Lipofectamine2000 (Invitrogen), with DNA lipid complexes formed
132 at a ratio of 2 μl/ 1 μg according to the manufacturer's instructions.
133
134 *Immunofluorescence analysis*
135 2.5 x 10^5 cells were grown on coverslips in 12-well culture plates, transfected 24 hr
136 later with 200 ng of PML plasmid plus either 200 ng Orf3 plasmid or empty vector,
137 and 24 hr later fixed for 10 min with 10% formalin in phosphate-buffered saline (PBS)
138 and permeabilized for 10 min with 0.5% Nonidet P40 in PBS. After blocking non-
139 specific protein interactions with PBS containing 1% w/v bovine serum albumin for 1
140 hr, antigens were then detected by sequential 1 hr incubations with primary and
141 secondary antibodies as follows: FLAG-tagged proteins, mouse monoclonal antibody

142 M2 (Sigma) and AlexaFluor488 goat-anti-mouse IgG (Invitrogen); endogenous PML,
143 mouse monoclonal antibody PGM3 (Santa Cruz) and AlexaFluor488 goat-anti-mouse
144 IgG (Invitrogen); Ad5 E4 Orf3, rat monoclonal antibody 6A11 (Nevels et al., 1999)
145 and AlexaFluor546 goat-anti-rat IgG (Invitrogen). Bound antibodies or GFP were
146 imaged using a Leica SP5 confocal microscope, and data exported as TIF images.
147 All images presented are single z-sections through the centre of the nucleus.
148
149 *Co-immunoprecipitation and western blotting*
150 This was carried out as previously described (Hoppe et al., 2006). Briefly, 3.5×10^6
151 U2OS cells plated on 10 cm dishes were transfected 24 hr later with 4 μg of PML
152 plasmid or empty vector, together with 4 μg Orf3 plasmid. Cell extracts were
153 prepared 24 hr later, a portion was reserved for total protein analysis and the
154 remainder immunoprecipitated using covalently coupled FLAG-agarose (Sigma).
155 Antigens were detected in western blot analysis using, for Orf3, rat monoclonal
156 antibody 6A11 (Nevels et al., 1999) and, for FLAG-tagged PML, rabbit polyclonal
157 anti-M2 (Sigma).
158
159 *Predictors of naturally disordered regions (PONDR®) analysis*
160 The PMLII sequence was analyzed for disorder propensity using the Predictor of
161 Natural Disordered Regions VLXT (PONDR®) (Romero et al., 2001, Romero et al.,
162 1997) provided by Molecular Kinetics (Indianapolis, IN) and the VSL2 disorder
163 predictor (Obradovic et al., 2006) via web access at http://www.pondr.com and
164 http://www.ist.temple.edu/disprot/predictorVSL2.php, respectively. Regions with the
165 potential to undergo disorder to order structural transitions upon binding to a partner,
166 termed Molecular Recognition Elements (MoREs) (Oldfield et al., 2005) or Molecular

Recognition Features (MoRFs) (Mohan et al., 2006), are indicated by sharp downward spikes (order propensity) flanked by regions of disorder (PONDR scores > 0.5). (PONDR® is copyright© 2004 by Molecular Kinetics, all rights reserved.)

Pml gene homology alignments

GenBank was searched for annotated PML genes and then for DNA sequences homologous to human *pml* exon 7a. This sequence was chosen as a search target because it encodes SUMO binding (Shen et al., 2006) and degron motifs (Scaglioni et al., 2006) that were likely to be well conserved between species. Full or partial *pml* gene sequences were identified from ten placental and one marsupial mammal species (*Homo sapiens*: NT_010194; *Pan troglodytes*: NW_001225242; *Macaca mulatta*: NW_001121176; *Canis familiaris*: NW_876294; *Felis catus*: AANG01142599; *Mus musculus*: NW_039474; *Rattus norvegicus*: NW_001084873; *Bos taurus*: NW_001494037; *Equus caballus*: NW_001799682; *Sus scrofa*: NW_001886480; *Monodelphis domestica*: NW_001581855). Sequences were manually aligned (MegAlign module, DNAStar), anchored on their homology to human exon 7a. In human *pml*, the 5’ end of exon 7b, which encodes the C-terminal 259 residues of PMLII, lies 642 bp from the 3’ end of exon 7a. Splice acceptor sites and open reading frames (ORF) able to encode proteins with clear homology to human PMLII were found in very similar positions (636-674 bp from 7a) in seven cases. Of the remaining sequences, homology to the 5’ end of human exon 7b was found in mouse and rat (1332, 1171 bp from 7a) but the ORFs were scrambled by frame shifting mutations, while opossum had only a short intron from exon 7a to 8a (1966 bp compared with 7.5 – 10.7 kbp) with no discernable homology to exon 7b. Eight predicted exon 7b-encoded polypeptides were aligned using the ClustalV

192 method. This alignment introduced two 2-position gaps into the 259 residue human
193 PMLII sequence.
194
195 **Results**
196 To show that the molecular target of E4 Orf3 within PML-NDs was PMLII, we
197 previously co-expressed Orf3 with specific PML isoforms, in either co-
198 immunoprecipitation or immunofluorescence colocalization analysis (Hoppe et al.,
199 2006). For the latter approach, we employed PML-null primary mouse embryo
200 fibroblasts, since similar analysis in human cells was complicated by the presence of
201 endogenous PMLs with which the transfected PML isoform could hetero-oligomerize.
202 In order to test the interaction of transiently expressed PML variants with Orf3 in
203 PML-containing human cells in this study, advantage was taken of the observation
204 that the RBCC motif within the common N-terminus of the nuclear PML isoforms (Fig.
205 1A) is necessary for these proteins to participate in PML-ND formation (Fagioli et al.,
206 1998). FLAG-tagged PML I – VI lacking this motif were tested for their localization in
207 U2OS cells either without or with coexpressed Orf3. All six ΔRBCC variants
208 displayed an identical exclusively diffuse nuclear fluorescence when expressed alone,
209 despite U2OS cells containing prominent PML-NDs formed of endogenous PML
210 proteins (Fig. 1B, C and data not shown). This contrasts with the behaviour of the
211 full-length isoforms, which are each recruited efficiently into PML-NDs (Beech et al.,
212 2005). When Orf3 was co-expressed with these proteins, only PMLIIΔRBCC was
213 relocalized into tracks with Orf3 (Fig. 1D, E and data not shown), as expected from
214 the earlier study. This result further showed that residues 1-360 of PMLII were
215 dispensable for its interaction with Orf3.
216

217 In order to further define the PML sequences involved in Orf3 binding, a set of four
218 in-frame deletions (Δ1-Δ4) was constructed in the unique C-terminal domain of
219 FLAG-PMLIIΔRBCC. To inform the design of these deletions, three PMLII sequences
220 annotated in GenBank databases, from human, chimpanzee and rhesus macaque,
221 were compared. These sequences are highly conserved, but regions of lower
222 conservation were identified and chosen as deletion end-points since these might be
223 expected to lie between functional elements of the sequence (Fig. 2A). During
224 construction of these mutations, we applied PONDR® analysis to further inform
225 mutational planning. This method predicts protein interaction motifs in protein
226 sequence, based on the observation that proteins that are capable of multiple
227 interactions are frequently highly disordered and that within this disorder there are
228 short sequences that are predicted to have a propensity to adopt ordered structure.
229 Well-defined dips in VLXT disorder prediction curves within disordered regions
230 (disorder scores > 0.5) can indicate short regions of order propensity (molecular
231 recognition elements, MoRE) that undergo disorder-to-order transitions upon binding
232 to a partner. Previous studies have validated the use of these distinctive downward
233 spikes in VLXT prediction curves to locate functional binding regions (Oldfield et al.,
234 2005). The structural propensity of these short regions can be translated into stable
235 structure by interaction with an interacting partner (Bourhis et al., 2004, Callaghan et
236 al., 2004, Longhi et al., 2003).

237

238 The unique C-terminal sequence of PMLII, from amino acid 571, was analysed by
239 two PONDR® tools generating predictions VLXT and VSL2. The VLXT prediction
240 (Fig. 2B) identified three potential MoREs within a region of predicted disorder that
241 covered the entire PMLII C-terminal unique region, while the VSL2 prediction (which

242 is based on a different and larger set of known structured and unstructured proteins)
243 showed MoREs 1 and 2 as part of a single region of increased order propensity (Fig.
244 2C). By contrast, the PML I C-terminus was predicted to be more ordered with no
245 MoREs (Fig. 2C), consistent with the fact that that this method of analysis is useful
246 for finding sites of interaction within regions that are predominantly disordered but not
247 within ordered regions. PMLII MoRE1 lay within the Δ1 mutation while MoRE3 was
248 contained within Δ2; MoRE2 spanned the junction between Δ1 & Δ2.

249

250 The ability of PMLII ΔRBCC variants Δ1- Δ4 to associate with Orf3 was assessed by
251 fluorescence co-localization. All four mutated proteins showed diffuse nuclear
252 fluorescence when expressed alone (Fig. 2D, F, H, J). When co-expressed with Orf3,
253 Δ3 and Δ4 showed complete co-localization in all cells (Fig. 2I, K) while Δ1 gave only
254 diffuse nuclear fluorescence, lacking any colocalization ability (Fig. 2E). Δ2 showed
255 an intermediate phenotype (Fig. 2G), with some cells demonstrating complete
256 colocalization (Fig. 2G inset) while the majority showed some colocalized tracks but
257 with considerable residual diffuse nuclear fluorescence, suggesting that the ability of
258 Δ2 to bind to Orf3 was impaired but not completely abrogated. Thus, PML residues
259 615-684, including MoRE1 and part of MoRE2, are necessary for Orf3 binding while
260 sequences C-terminal of residue 685, including MoRE3, are not essential.

261

262 To map more precisely the sequences of PMLII necessary for the Orf3 interaction,
263 and in the light of the PONDR® predictions (Fig. 2B, C), five further in-frame
264 deletions were constructed in the PMLII C-terminus (Fig. 3A), removing either
265 subsections of the region deleted in Δ1 (Δ7, Δ8, Δm1), or the MoRE2 motif

266 overlapping the boundary of Δ1 and Δ2 (Δm2); Δm1 & Δm2 were also combined in a
267 double mutant (Δm1m2). When tested in the fluorescence co-localization assay, Δ8
268 and Δm2 strongly associated with Orf3 tracks (Fig. 3B, E) while Δm1, Δ7 and Δm1m2
269 were essentially unable to do so (Fig. 3C, D and data not shown); faint tracks of Δ7
270 were sometimes seen, but in contrast to Δ8 and Δm2 these only partially co-localized
271 with Orf3. These data mapped the Orf3 interaction motif in PMLII to residues 645-674,
272 with a possible supporting involvement of adjacent sequences from the properties of
273 mutant Δ2 (Fig. 2G). This mapped region coincides almost exactly with the region of
274 potential induced order (MoRE1/2) predicted in PMLII by PONDR® VLXT and VSL2
275 (Fig. 2B, C).

276

277 To confirm that the induction of PML variant localization into Orf3-colocalized tracks
278 was an indication of protein : protein interaction between these two partners, co-
279 immunoprecipitation analysis was performed (Fig. 4). Each of the PML variants
280 tested was efficiently expressed and precipitated by anti-FLAG agarose beads (Fig.
281 4A). However, although expression of Orf3 in the extracts was broadly equivalent
282 across all samples (Fig. 4B), the amounts of Orf3 co-precipitated with the various
283 FLAG-PMLs varied greatly (Fig. 4C). As expected, II ΔRBCC co-precipitated
284 significant amounts of Orf3 (lane 4) while I ΔRBCC, included as a negative control,
285 did not (lane 3). The Δ1, Δm1, Δm1m2 and Δ7 variants of II ΔRBCC did not co-
286 precipitate Orf3 at all (lanes 5, 9, 11, 12), consistent with the fact that these variants
287 also failed to relocalize into tracks when coexpressed with Orf3 (Figs. 2, 3 and data
288 not shown). The other variants tested: Δ2, Δ3, Δ4, Δ8 and Δm2, each of which was
289 able to associate with Orf3 by fluorescence analysis, also co-precipitated Orf3, in the
290 case of Δ3 & Δ4 more efficiently than did the wild-type sequence. These results

291 therefore confirm that PMLII residues 645-674, comprising the sequence deleted in
292 Δm1 plus Δ7, are required for Orf3 binding.
293
294 To determine if these essential sequences from PMLII were also sufficient for Orf3
295 binding, PMLII residues 645-684, comprising MoRE1 and sequences C-terminal to it
296 up to the original Δ1 boundary within MoRE2, were transferred onto the C-terminus
297 of hrGFP that was tagged with the nuclear localization signal from SV40 large T
298 antigen to direct the protein to the nucleus; as expected, the location of this protein
299 was unaffected by co-expression of Orf3 (Fig. 5A). Addition of the PMLII sequences
300 caused the hrGFP fusion, expressed alone, to quantitatively relocalize into structures
301 that had the appearance of nucleoli (Fig. 5B). However, when Orf3 was co-expressed
302 with this construct, a substantial fraction of the fusion protein was drawn back out of
303 these structures into co-localization with Orf3 tracks (Fig. 5C), indicating that PMLII
304 residues 645-684 were sufficient for Orf3 interaction and could function
305 autonomously from the rest of the protein.
306
307 Having defined the Orf3-binding element in PMLII, we were interested to determine
308 whether either its amino acid sequence or the position of MoREs within it was
309 conserved among the PML proteins of different species. Seven of ten PML genes
310 identified in database searches could be predicted to encode homologues of human
311 PMLII. Of the other three, the exon 7b sequences in mouse and rat were non-
312 functional, in agreement with experimental data for the mouse (Condemine et al.,
313 2006), while the opossum sequence lacked exon 7b completely. The extent of
314 homology at each position in an alignment of human PMLII with these seven
315 predicted PMLII C-terminal domains is represented in Fig. 6A. Only 27% of 263

316 positions were identical across seven or all eight of the sequences. This compares
317 with 63% of 267 positions in a similar alignment of predicted PML I C-terminal
318 domains (substituting murine PML for feline PML sequence, since the feline exon 9
319 sequence was not available; data not shown). Thus the unique sequences of PMLII
320 that are targeted by Ad5 are relatively poorly conserved in PML. Moreover, the
321 mapped Orf3 interaction sequence in PMLII did not coincide with the region of
322 highest conservation (Fig. 6A, arrow).
323
324 PONDR® VLXT analyses were then run for the predicted bovine (Fig. 6B) and canine
325 (Fig. 6C) PMLII C-termini. Despite the low sequence identity between the bovine and
326 human sequences (45% of 244 aligned positions where both have residues), three
327 MoREs were predicted in bovine PMLII at positions very similar to those identified in
328 the human protein. The canine PMLII exon 7b-encoded sequence is significantly
329 shorter than the human form, being truncated at position 210 in the alignment. It too
330 was predicted to contain several potential protein interaction sites, although their
331 precise positions differed from those predicted for the human and bovine PMLII
332 MoREs.
333
334 **Discussion**
335 The Ad5 E4 Orf3 protein is required for the disruption of PML-NDs. This Orf3 function
336 requires it to interact with PML isoform II (Hoppe et al., 2006), a major component
337 within the population of PML species in the cell (Condemine et al., 2006). In this
338 study, we have shown that the target for Orf3 binding is a 40 residue sequence within
339 PMLII. Deletion of this sequence destroys the interaction with Orf3 whilst its transfer
340 to a heterologous protein confers Orf3 interaction properties in an *in vivo* assay. The

341 interacting PML sequence, residues 645-684, is encoded by exon 7b of the *pml* gene
342 and is thus unique to PMLII among nuclear PML species, in full agreement with the
343 observation that only this PML isoform can interact with Orf3.
344
345 The Orf3 binding sequence of PMLII was defined using cDNA clones deleted for the
346 RBCC motif. The encoded proteins therefore lack the ability to heteroligomerize
347 (Peng et al., 2002) and so cannot be indirectly recruited into association with Orf3 via
348 PML:PML interactions. As expected, they completely failed to localize into PML-NDs
349 (Borden et al., 1996), even though this cell type contained clearly defined PML-ND
350 structures formed of endogenous PML with which the heterologous proteins were
351 free to interact. Among the six nuclear PML isoforms, only the PMLII ΔRBCC
352 derivative could associate with Orf3 in immunofluorescence or co-
353 immunoprecipitation assays, in agreement with our previous study using full-length
354 PMLII (Hoppe et al., 2006) and indicating that the association of PMLII with PML-NDs
355 is not necessary for its interaction with Orf3.
356
357 The various deletion variants of PMLII that retained Orf3 interaction ability did not
358 always appear equivalent in activity. Although the fluorescence co-localization assay
359 is not quantitative, it was consistently observed that the Δ3 and Δ4 mutants were
360 very effectively brought into Orf3 tracks as compared with the Δ2 mutant and even
361 the undeleted PMLII C-terminus. These same proteins were also more effective in
362 co-precipitating Orf3. These data suggest that the C-terminal 70 residues of PMLII
363 may exert a negative effect on its binding to Orf3. The other mutants that retained
364 Orf3 interaction function, Δ2, Δ8 and Δm2, all appeared to be less efficiently recruited
365 to Orf3 tracks, and for Δ8 and Δm2 this was supported by reduced co-

366 immunoprecipitation of Orf3. Thus the activity of the core Orf3 binding element in
367 PMLII may be enhanced by its flanking sequences.
368
369 The use of deleted protein variants to map protein interactions has the caveat that
370 such deletions may cause gross changes to the structure of the folded protein and
371 hence impact on functions that are actually encoded elsewhere in the polypeptide. All
372 of the C-terminally deleted PMLII variants used in the study accumulated to similar
373 levels to undeleted PMLII, as judged by the strength of bands in western blot analysis
374 of total protein and the typical fluorescent intensity of individual expressing cells
375 examined by immunofluorescence. Both these observations indicate that the deleted
376 PMLII species were not destabilised relative to full length protein and hence are not
377 likely to be grossly altered in structure. The ability to express deleted forms of PMLII
378 without such problems being manifest is likely due to the predicted disordered nature
379 of the entire C-terminal domain.
380
381 The addition of the Orf3 interaction motif of PMLII onto hrGFP conferred apparent
382 nucleolar targeting on the protein. PML has been shown previously to be induced into
383 nucleolar localization by either DNA damage or inhibition of the proteasome
384 (Bernardi et al., 2004, Mattsson et al., 2001) or to associate with nucleoli during
385 normal growth of non-transformed cells (Janderovd-Rossmeislova et al., 2007). It is
386 conceivable that our study has identified an element that contributes to this nucleolar
387 targeting of endogenous PML proteins. However, it was shown recently that direct
388 nucleolar targeting of PML was largely restricted to PML isoforms I and IV
389 (Condemine et al., 2007). Hence it is more probable that the nucleolar localization of

390 hrGFP-M1M2 protein observed here results from the generation of activity through
391 the transfer of this protein sequence into a heterologous context.
392
393 Orf3 reorganizes several cellular proteins in addition to PML, including RBCC family
394 member TIF1α, which directly binds Orf3 (Yondola & Hearing, 2007), and the MRN
395 complex comprising Mre11, Rad50, and Nbs1 (Stracker et al., 2002). The direct
396 binding partner for Orf3 within MRN has not been determined, although Nbs1 is
397 dispensable for Orf3 to relocalize Rad50 and Mre11 (Araujo et al., 2005). The Orf3
398 sequence requirements for interaction with PML, MRN and TIF1α are very similar,
399 suggesting that the Orf3-interaction sites in these proteins might be sequence-related.
400 Homology matches to the 40 residue Orf3-interaction motif from PMLII were
401 identified in both Rad50 and TIF1α (Fig. 7). The significance of the Rad50 match is
402 unclear, but the TIF1α match is clearly better than achieved in comparisons with two
403 irrelevant proteins of similar length (T antigen, L4 100K). Moreover, the sequence
404 match lies at the C-terminal end of the TIF1α RBCC domain, which has been shown
405 to mediate Orf3 binding (Yondola & Hearing, 2007). Finally, the corresponding
406 sequence from its Orf3 non-interacting relative TIF1β (Yondola & Hearing, 2007) is
407 significantly less similar to the PMLII Orf3 binding motif (Fig. 7). These strands of
408 argument support the possibility that sequence relatedness with PMLII can predict
409 the Orf3 binding site in TIF1α.
410
411 In addition to forming nuclear tracks, Orf3 also localizes to perinuclear cytoplasmic
412 structures identified as aggresomes (Araujo et al., 2005) and participates in
413 delivering MRN complex to these structures for inactivation and degradation (Araujo
414 et al., 2005, Liu et al., 2005). Here, Orf3 aggresomes were observed in only a

415 minority of expressing cells. PML species unable to bind Orf3 never co-localized in
416 these structures (e.g. Fig. 1D) while those variants able to bind Orf3 associated with
417 aggresomes only in a few cells expressing high levels of the PML construct (data not
418 shown). These data are consistent with the report that endogenous PML does not
419 localize with Orf3 in aggresomes (Araujo et al., 2005).
420
421 The mapped binding site for Orf3 in PMLII was found to be relatively poorly
422 conserved between PML proteins of different species. Exon 7b, which encodes the
423 unique portion of PMLII, was only found intact in a subset of species for which data
424 was available, and for those species able to encode PMLII, its isoform-specific C-
425 terminal sequence was considerably less well conserved than the equivalent region
426 of PML I. Moreover, even within the PMLII C-terminus, the mapped interaction site
427 was not the most conserved part of the sequence. These findings suggest that Ad5
428 Orf3 may not be able to interact widely with the PML proteins of other species.
429 However, both the two non-human PMLII sequences for which PONDR® analysis
430 was carried out were predicted to contain MoREs and, for the bovine sequence, the
431 position of these predicted elements was very similar to those predicted for human
432 PMLII. Thus, it may be that Orf3 recognizes a shape or structure in PML rather than
433 a highly specific sequence, in which case it may have wider cross-species binding
434 reactivity than the sequence homology analysis suggests. Whether Ad5 Orf3 can
435 bind specifically to PMLII from other species remains to be tested.
436
437 Adenoviruses have been isolated from a wide range of animal species. Whilst these
438 viruses retain the overall genome organization of the human Ads, including a
439 presumptive E4 gene at the genome right end with multiple open reading frames,

440 outside of the simian Ads it is not possible to identify definitive functional homologues
441 of human Ad E4 Orf3 by sequence comparison. Thus, the host target(s) of Orf3 might
442 be expected also to be quite divergent, assuming function has been conserved
443 during the co-evolution of these viruses with their respective hosts. Given that the
444 disruption of PML-NDs by Orf3 combats an intrinsic or innate antiviral response in
445 human and primate cells (Ullman & Hearing, 2008, Ullman et al., 2007), it will be
446 interesting to explore the function of Ad5 Orf3 in other host species.
447
448 PONDR® analysis identified three potential protein interaction sites (MoREs) within
449 the C-terminal domain of human PMLII, one of which (MoRE1) formed the core of the
450 Orf3-binding sequence subsequently identified. This study therefore demonstrates
451 the potential for predicting functional protein binding sites within unstructured
452 polypeptide sequence by this method. The MoRE1 motif is unlikely to have evolved
453 within PMLII to provide an interaction site for Orf3, given that the ability of the virus to
454 make this interaction with the host can be seen as favouring the replication of virus
455 and hence is likely to be deleterious to the host. Instead, it and the other two
456 predicted MoREs are likely to have one or more endogenous cellular partners. The
457 experimentally demonstrated ability of the C-terminal MoRE of p53 to bind four
458 different partners (Oldfield et al., 2008) serves as a model for how a viral protein
459 could usurp an endogenous MoRE-mediated binding interaction and thereby alter
460 normal cellular communication or protein function. Although MoREs do exhibit
461 different degrees of specificity, their minimal binding determinants facilitate
462 promiscuity. If MoRE1 does have an endogenous partner, then its displacement by
463 Ad5 Orf3 could contribute to the observed phenotype in relieving the antiviral
464 response or to additional, as yet undetermined, phenotypes.

465

466 **Acknowledgements**

467 The authors gratefully acknowledge the assistance of G. Scott with cell culture and
468 the DNA sequencing service provided by L. Ward, S. Davis and H. Brown in the
469 Molecular Biology Core Facility, Department of Biological Sciences, University of
470 Warwick. Monoclonal antibody specific for Ad5 E4 Orf3 was generously provided by
471 Dr T. Dobner, Heinrich Pette Inst Expt Virol & Immunol, Martinistr 52, D-20251
472 Hamburg, Germany. This work was supported by grants from the Biotechnology and
473 Biological Sciences Research Council to KNL and to TR, from the AICR to MC.

474

475 **References**

476 Araujo, F. D., Stracker, T. H., Carson, C. T., Lee, D. V. & Weitzman, M. D. (2005).
477 Adenovirus type 5 E4orf3 protein targets the Mre11 complex to cytoplasmic
478 aggresomes. *Journal of Virology* **79**, 11382-11391.
479 Beech, S. J., Lethbridge, K. J., Killick, N., McGlincy, N. & Leppard, K. N. (2005).
480 Isoforms of the promyelocytic leukemia protein differ in their effects on ND10
481 organization. *Experimental Cell Research* **307**, 109-117.
482 Bernardi, R. & Pandolfi, P. P. (2007). Structure, dynamics and functions of
483 promyelocytic leukaemia nuclear bodies. *Nature Reviews Molecular Cell*
484 *Biology* **8**, 1006-1016.
485 Bernardi, R., Scaglioni, P. P., Bergmann, S., Horn, H. F., Vousden, K. H. & Pandolfi,
486 P. P. (2004). PML regulates p53 stability by sequestering Mdm2 to the
487 nucleolus. *Nature Cell Biology* **6**, 665-672.
488 Borden, K. L. B., Lally, J. M., Martin, S. R., O'Reilly, N. J., Solomon, E. & Freemont,
489 P. S. (1996). In vivo and in vitro characterization of the B1 and B2 zinc-

490 binding domains from the acute promyelocytic leukemia protooncoprotein PML.
491 *Proceedings of the National Academy of Sciences of the United States of*
492 *America* **93**, 1601-1606.
493 Bourhis, J. M., Johansson, K., Receveur-Brechot, V., Oldfield, C. J., Dunker, A. K.,
494 Canard, B. & Longhi, S. (2004). The C-terminal domain of measles virus
495 nucleoprotein belongs to the class of intrinsically disordered proteins that fold
496 upon binding to their physiological partner. *Virus Research* **99**, 157-167.
497 Callaghan, A. J., Aurikko, J. P., Ilag, L. L., Grossman, J. G., Chandran, V., Kuhnel, K.,
498 Poljak, L., Carpousis, A. J., Robinson, C. V., Symmons, M. F. & Luisi, B. F.
499 (2004). Studies of the RNA degradosome-organizing domain of the
500 Escherichia coli ribonuclease RNase E. *Journal of Molecular Biology* **340**,
501 965-979.
502 Carvalho, T., Seeler, J. S., Ohman, K., Jordan, P., Pettersson, U., Akusjarvi, G.,
503 Carmofonseca, M. & Dejean, A. (1995). Targeting of adenovirus E1A and E4-
504 ORF3 proteins to nuclear matrix-associated PML bodies. *Journal of Cell*
505 *Biology* **131**, 45-56.
506 Condemine, W., Takahashi, Y., Le Bras, M. & de The, H. (2007). A nucleolar
507 targeting signal in PML-I addresses PML to nucleolar caps in stressed or
508 senescent cells. *Journal of Cell Science* **120**, 3219-3227.
509 Condemine, W., Takahashi, Y., Zhu, J., Puvion-Dutilleul, F., Guegan, S., Janin, A. &
510 de The, H. (2006). Characterization of endogenous human promyelocytic
511 leukemia isoforms. *Cancer Research* **66**, 6192-6198.
512 Doucas, V., Ishov, A. M., Romo, A., Juguilon, H., Weitzman, M. D., Evans, R. M. &
513 Maul, G. G. (1996). Adenovirus replication is coupled with the dynamic
514 properties of the PML nuclear structure. *Genes & Development* **10**, 196-207.

515 Evans, J. D. & Hearing, P. (2003). Distinct roles of the adenovirus E4 ORF3 protein
516 in viral DNA replication and inhibition of genome concatenation. *Journal of*
517 *Virology* **77**, 5295-5304.
518 Everett, R. D. & Chelbi-Alix, M. K. (2007). PML and PML nuclear bodies: Implications
519 in antiviral defence. *Biochimie* **89**, 819-830.
520 Everett, R. D. & Maul, G. G. (1994). HSV-1 IE protein Vmw110 causes redistribution
521 of PML. *EMBO Journal* **13**, 5062-5069.
522 Everett, R. D. & Murray, J. (2005). ND10 components relocate to sites associated
523 with herpes simplex virus type 1 nucleoprotein complexes during virus
524 infection. *Journal of Virology* **79**, 5078-5089.
525 Everett, R. D., Parada, C., Gripon, P., Sirma, H. & Orr, A. (2008). Replication of
526 ICP0-Null mutant herpes simplex virus type 1 is restricted by both PML and
527 Sp100. *Journal of Virology* **82**, 2661-2672.
528 Everett, R. D., Rechter, S., Papior, P., Tavalai, N., Stamminger, T. & Orr, A. (2006).
529 PML contributes to a cellular mechanism of repression of herpes simplex virus
530 type 1 infection that is inactivated by ICP0. *Journal of Virology* **80**, 7995-8005.
531 Fagioli, M., Alcalay, M., Pandolfi, P. P., Venturini, L., Mencarelli, A., Simeone, A.,
532 Acampora, D., Grignani, F. & Pelicci, P. G. (1992). Alternative splicing of PML
533 transcripts predicts expression of several carboxyterminally different protein
534 isoforms. *Oncogene* **7**, 1083-1091.
535 Fagioli, M., Alcalay, M., Tomassoni, L., Ferrucci, P. F., Mencarelli, A., Riganelli, D.,
536 Grignani, F., Pozzan, T., Nicoletti, I., Grignani, F. & Pelicci, P. G. (1998).
537 Cooperation between the RING+B1-B2 and coiled-coil domains of PML is
538 necessary for its effects on cell survival. *Oncogene* **16**, 2905-2913.

539 Hoppe, A., Beech, S. J., Dimmock, J. & Leppard, K. N. (2006). Interaction of the
540 adenovirus type 5 E4 Orf3 protein with promyelocytic leukemia protein isoform
541 II is required for ND10 disruption. *Journal of Virology* **80**, 3042-3049.
542 Ishov, A. M. & Maul, G. G. (1996). The periphery of nuclear domain 10 (ND10) as
543 site of DNA virus deposition. *Journal of Cell Biology* **134**, 815-826.
544 Janderovd-Rossmeislova, L., Novakova, Z., Vlasakova, J., Phillmonenko, V., Hozak,
545 P. & Hodny, Z. (2007). PML protein association with specific nucleolar
546 structures differs in normal, tumor and senescent human cells. *Journal of*
547 *Structural Biology* **159**, 56-70.
548 Jensen, K., Shiels, C. & Freemont, P. S. (2001). PML protein isoforms and the
549 RBCC/TRIM motif. *Oncogene* **20**, 7223-7233.
550 Kalderon, D., Roberts, B. L., Richardson, W. D. & Smith, A. E. (1984). A short amino-
551 acid sequence able to specify nuclear location. *Cell* **39**, 499-509.
552 Kelly, C., van Driel, R. & Wilkinson, G. W. G. (1995). Disruption of PML-associated
553 nuclear bodies during human cytomegalovirus infection. *Journal of General*
554 *Virology* **76**, 2887-2893.
555 Leppard, K. N. & Dimmock, J. (2006). Virus interactions with PML nuclear bodies. In
556 *Viruses and the Nucleus*, pp213-245. Edited by J. Hiscox: J Wiley.
557 Liu, Y., Shevchenko, A. & Berk, A. J. (2005). Adenovirus exploits the cellular
558 aggresome response to accelerate inactivation of the MRN complex. *Journal*
559 *of Virology* **79**, 14004-14016.
560 Longhi, S., Receveur-Brechot, V., Karlin, D., Johansson, K., Darbon, H., Bhella, D.,
561 Yeo, R., Finet, S. & Canard, B. (2003). The C-terminal domain of the measles
562 virus nucleoprotein is intrinsically disordered and folds upon binding to the C-

563 terminal moiety of the phosphoprotein. *Journal of Biological Chemistry* **278**,
564 18638-18648.
565 Mattsson, K., Pokrovskaja, K., Kiss, C., Klein, G. & Szekely, L. (2001). Proteins
566 associated with the promyelocytic leukemia gene product (PML)-containing
567 nuclear body move to the nucleolus upon inhibition of proteasome-dependent
568 protein degradation. *Proceedings of the National Academy of Sciences of the*
569 *United States of America* **98**, 1012-1017.
570 Mohan, A. C., Oldfield, C. J., Radivojac, P., Vacic, V., Cortese, M. S., Dunker, A. K. &
571 Uversky, V. N. (2006). Analysis of molecular recognition features (MoRFs).
572 *Journal of Molecular Biology*, 1043-1059.
573 Nevels, M., Tauber, B., Kremmer, E., Spruss, T., Wolf, H. & Dobner, T. (1999).
574 Transforming potential of the adenovirus type 5 E4orf3 protein. *Journal of*
575 *Virology* **73**, 1591-1600.
576 Obradovic, D., Peng, K., Vucetic, S., Radivojac, P. & Dunker, A. K. (2006).
577 Heterogeneous sequence properties improves prediction of protein disorder.
578 *Proteins - Structure, Function & Genetics* **61(S7)**, 176-182.
579 Oldfield, C. J., Cheng, Y., Cortese, M. S., Romero, P., Uversky, V. N. & Dunker, A. K.
580 (2005). Coupled folding and binding with alpha-helixforming molecular
581 recognition elements. *Biochemistry* **44**, 12454-12470.
582 Oldfield, C. J., Meng, J., Yang, J. Y., Yang, M. Q., Uversky, V. N. & Dunker, A. K.
583 (2008). Flexible nets: disorder and induced fit in the associations of p53 and
584 14-3-3 with their partners. **9 (suppl 1)**, S1.
585 Peng, H. Z., Feldman, I. & Rauscher, F. J. (2002). Hetero-oligomerization among the
586 TIF family of RBCC/TRIM domain-containing nuclear cofactors: A potential

587 mechanism for regulating the switch between coactivation and corepression.
588 *Journal of Molecular Biology* **320**, 629-644.
589 Romero, P., Obradovic, D., Li, X., Garner, E. C., Brown, C. J. & Dunker, A. K. (2001).
590 Sequence complexity of disordered protein. *Proteins - Structure, Function &*
591 *Genetics* **42**, 38-48.
592 Romero, P., Obradovic, Z., Kissinger, C. R., Villafranca, J. E. & Dunker, A. K. (1997).
593 Identifying disordered regions in proteins from amino acid sequences. In *IEEE*
594 *International Conference on Neural Networks*, pp. 90-95.
595 Salomoni, P. & Bellodi, C. (2007). New insights into the cytoplasmic function of PML.
596 *Histology and Histopathology* **22**, 937-946.
597 Scaglioni, P. P., Yung, T. M., Cai, L. F., Erdjument-Bromage, H., Kaufman, A. J.,
598 Singh, B., Teruya-Feldstein, J., Tempst, P. & Pandolfi, P. P. (2006). A CK2-
599 dependent mechanism for degradation of the PML tumor suppressor. *Cell* **126**,
600 269-283.
601 Shen, T. H., Lin, H.-K., Scaglioni, P. P., Yung, T. M. & Pandolfi, P. P. (2006). The
602 mechanisms of PML-nuclear body formation. *Molecular Cell* **24**, 331-339.
603 Sternsdorf, T., Jensen, K. & Will, H. (1997). Evidence for covalent modification of the
604 nuclear dot-associated proteins PML and Sp100 by PIC1/SUMO-1. *Journal of*
605 *Cell Biology* **139**, 1621-1634.
606 Stracker, T. H., Carson, C. T. & Weitzman, M. D. (2002). Adenovirus oncoproteins
607 inactivate the Mre11-Rad50-NBS1 DNA repair complex. *Nature* **418**, 348-352.
608 Stracker, T. H., Lee, D. V., Carson, C. T., Araujo, F. D., Ornelles, D. A. & Weitzman,
609 M. D. (2005). Serotype-specific reorganization of the Mre11 complex by
610 adenoviral E4orf3 proteins. *Journal of Virology* **79**, 6664-6673.

611 Ullman, A. J. & Hearing, P. (2008). The cellular proteins PML and Daxx mediate an
612 innate antiviral defence antagonized by the adenovirus E4 ORF3 protein.
613 *Journal of Virology* **82**, 7325-7335.
614 Ullman, A. J., Reich, N. C. & Hearing, P. (2007). Adenovirus E4 ORF3 protein inhibits
615 the interferon-mediated antiviral response. *Journal of Virology* **81**, 4744-4752.
616 Yondola, M. A. & Hearing, P. (2007). The adenovirus E4 ORF3 protein binds and
617 reorganizes the TRIM family member transcriptional intermediary factor 1
618 alpha. *Journal of Virology* **81**, 4264-4271.
619
620 **Figure Legends**
621 **Figure 1.** PMLII – Orf3 interaction does not require the RBCC motif. Panel A: A
622 schematic representation of PMLII (top) and its ΔRBCC variant (bottom). The RBCC
623 domain comprises Ring Finger (R), two zinc-binding B boxes (B) and a Coiled Coil
624 region (CC). Also indicated are the PML nuclear localisation signal (N), SUMO
625 binding site (S) and the three sites of covalent modification by SUMO1 (Su). The
626 FLAG epitope N-terminal extension is shown as a black box. Panels B – F:
627 Immunofluorescence analysis of U2OS cells either transfected with (B) FLAG-PML I
628 ΔRBCC or (C) FLAG-PMLII ΔRBCC and stained for FLAG (green) and DNA (DAPI,
629 blue), transfected with (D) FLAG-PML I ΔRBCC & Orf3 or (E) FLAG-PMLII ΔRBCC
630 and Orf3 and stained for FLAG (green) and Orf3 (red), or mock-transfected (F) and
631 stained for endogenous PML (green) and DNA (DAPI, blue). Scale bars,– 10 μm.
632
633 **Figure 2.** Delineation of the Orf3 binding site in the C-terminus of PMLII. (A) Amino
634 acid sequence alignment of the exon 7b sequences of PMLII from human (Hom),
635 chimpanzee (Pan) and Macaque (Mac); grey shaded regions indicate identity

636 between the three sequences. The beginning and end points of the in-frame deletion
637 mutations Δ1 – Δ4 generated in human PMLII cDNA are indicated below the
638 alignment. (B) PONDR® VLXT prediction for the C-terminal domain of PMLII,
639 showing the predicted molecular recognition elements (MoRE) 1 - 3 relative to
640 mutations Δ1 – Δ4. (C) PONDR® VLS2 prediction for the C-terminal domain of PMLII
641 (grey) and PML I (black). Panels D – K: Immunofluorescence analysis of U2OS cells
642 transfected with (D) FLAG-PMLIIΔ1 alone or (E) with Orf3, (F) FLAG-PMLIIΔ2 alone
643 or (G) with Orf3, (H) FLAG-PMLIIΔ3 alone or (I) with Orf3, (J) FLAG-PMLIIΔ4 alone
644 or (K) with Orf3, and stained for FLAG and Orf 3. Scale bar, panel D – 10 μm; all
645 panels at this magnification.
646
647 **Figure 3.** Co-localization of PMLII with Orf3 requires sequences from MoRE1. (A)
648 PMLII sequence across the MoRE1 & MoRE2 elements, showing the positions of
649 deletion mutations as indicated. Panels B – E: Immunofluorescence analysis of
650 U2OS cells transfected with Orf3 plus (B) PMLIIΔ8, (C) PMLIIΔm1, (D) PMLIIΔ7, (E)
651 PMLIIΔm2. Orf3 staining is shown on the left and FLAG (PML) staining on the right in
652 each panel. Scale bar, panel B – 10 μm; all panels at this magnification.
653
654 **Figure 4.** Interaction of PMLII sequence variants with Orf3 by co-immunoprecipitation
655 analysis. U2OS cells were co-transfected with Orf3 and FLAG-PML expression
656 plasmids as indicated at the top of the figure and cell extracts prepared for total
657 protein analysis and immunoprecipitation with anti-FLAG antibody. (A)
658 Immunoprecipitated FLAG-PML; (B) Orf3 in total extract; (C) Orf3 co-
659 immunoprecipitated with FLAG-PML. The migration positions of protein molecular
660 mass markers (kD) are shown at the right of each panel.

661

662 **Figure 5.** PMLII residues 645-684 are sufficient for Orf3 binding. U2OS cells were
663 transfected with (A) hrGFP-NLS plus Orf3, (B) hrGFP-NLS-m1m2 plus empty vector
664 or (C) hrGFP-NLS-m1m2 plus Orf3 and then stained for Orf3 (red) and DNA (DAPI,
665 blue). GFP fluorescence was visualised directly (green). Scale bar – 10 μm.

666

667 **Figure 6.** Sequence and structure conservation in PMLII. (A) Sequence conservation
668 across the predicted *pml* exon7b-encoded polypeptides from human, chimpanzee,
669 macaque, dog, cat, cow, horse and pig (see Methods for details). The bar height and
670 shading indicate the extent of homology at each position in the alignment, with the
671 maximum bar height shown representing identity across all eight sequences and the
672 next highest representing seven out of eight identity. The position of the 40 residue
673 Orf3-binding sequence is represented by a black arrow. (B and C) PONDR® VLXT
674 predictions for the predicted C-terminal domains of bovine (B) and canine (C) PMLII.

675

676 **Figure 7.** Homology alignments of the PMLII Orf3 binding motif with other proteins.
677 Protein sequences (GenBank: AAB07119 [Rad50]; NP_005582 [Mre11]; NP_056989
678 [TIF1α]; CAA66150 [TIF1β]) were analysed in pairwise alignments with the 40
679 residue Orf3 binding motif from PMLII (residues 645-684) using the Lipman-Pearson
680 method, DNAStar software (Ktuple 2; Gap Penalty 4; Gap Length Penalty 12).
681 Symbols "| : . " indicate identity and decreasing levels of similarity between each
682 sequence and the PMLII motif.

Figure 1

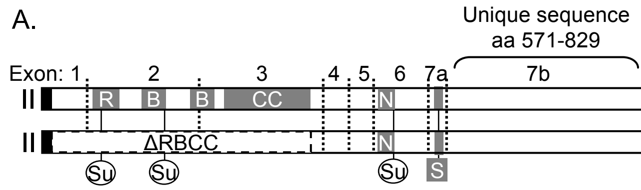

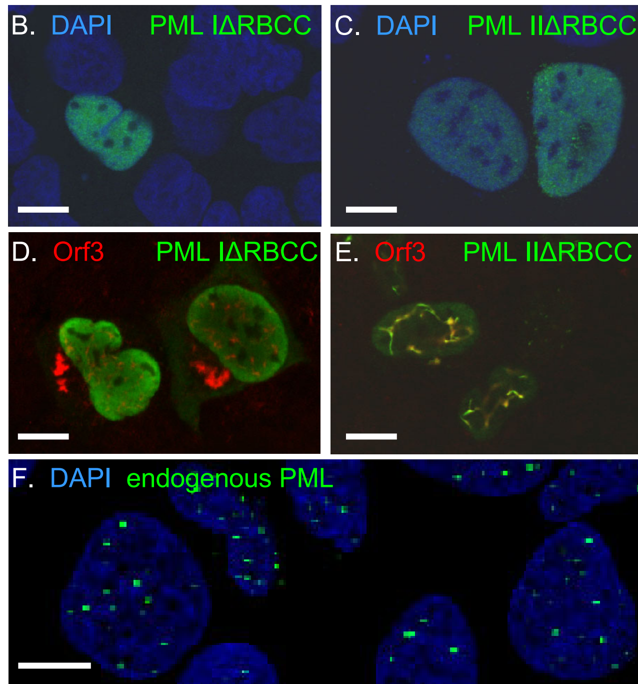

Figure 2

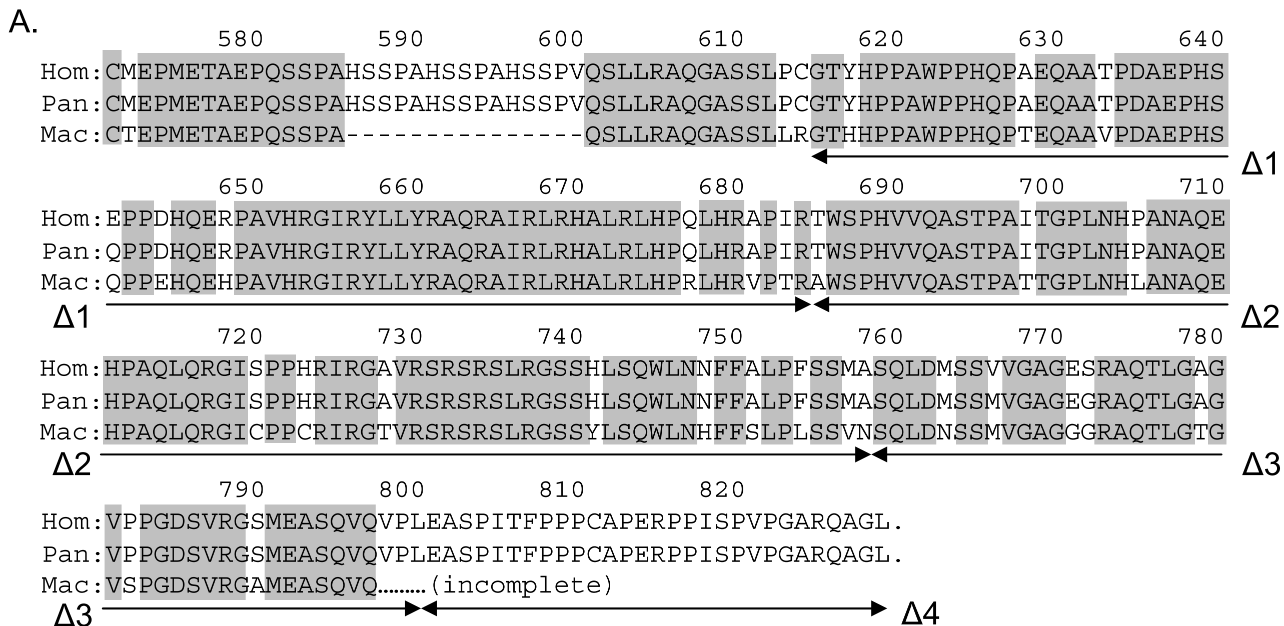

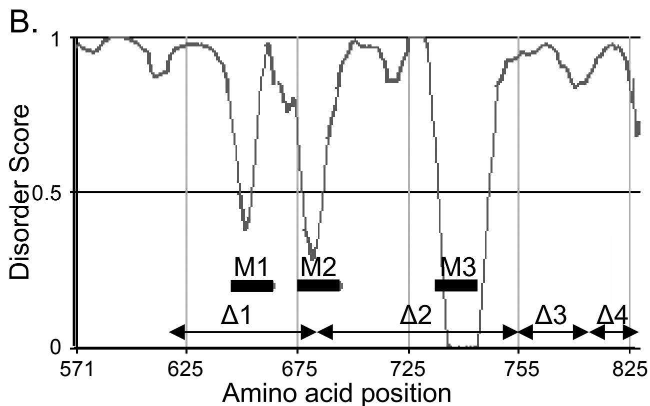

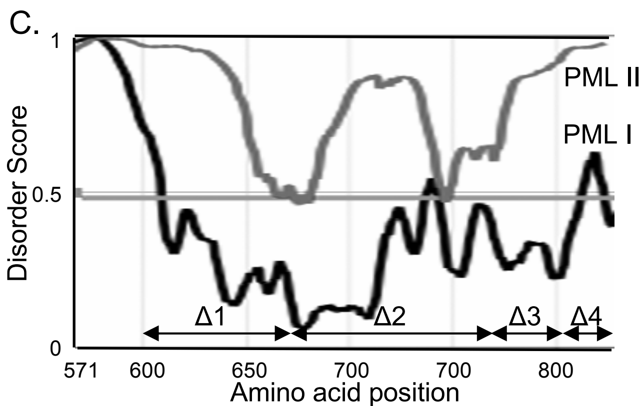

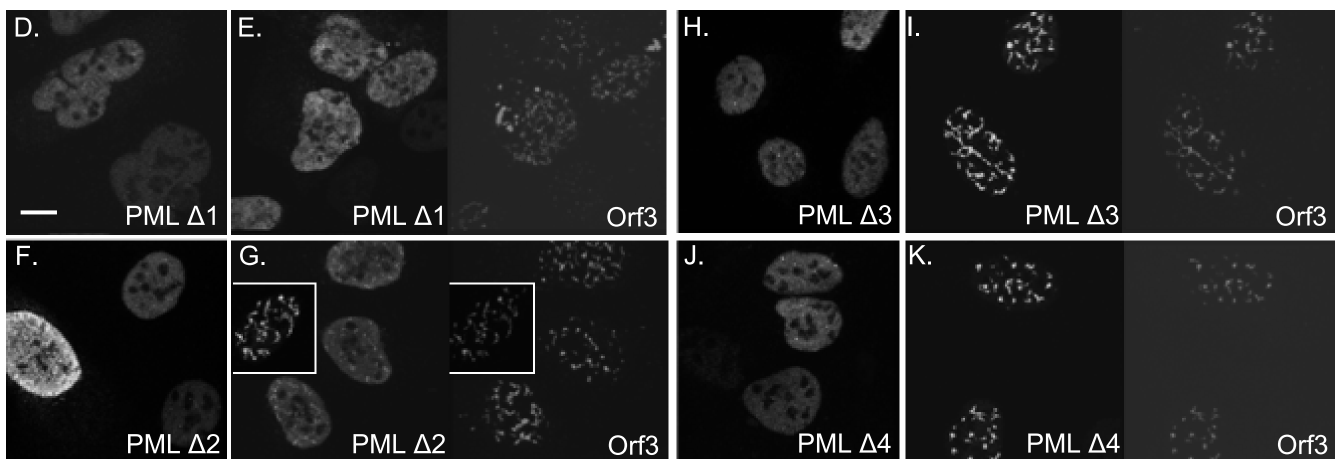

Figure 3

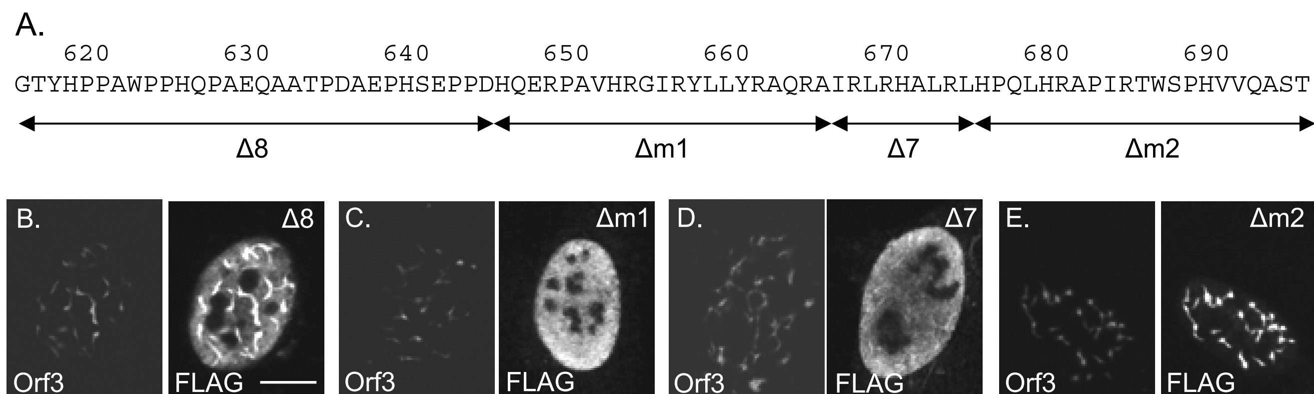

Figure 4

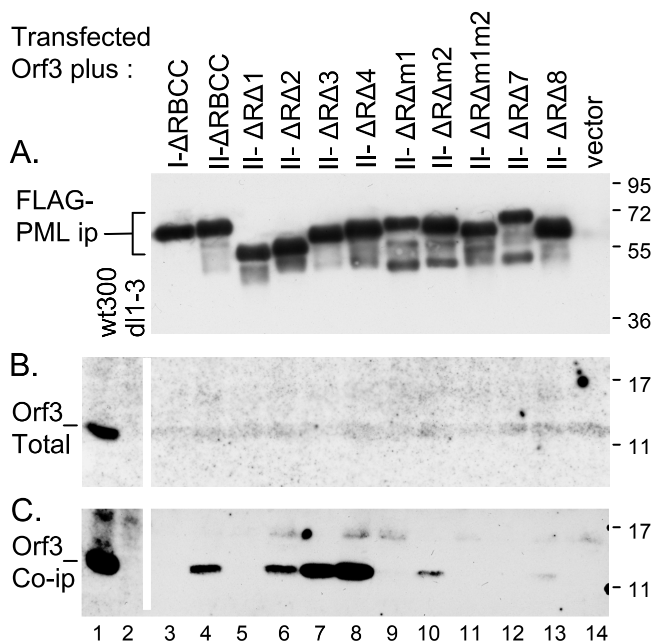

Figure 5

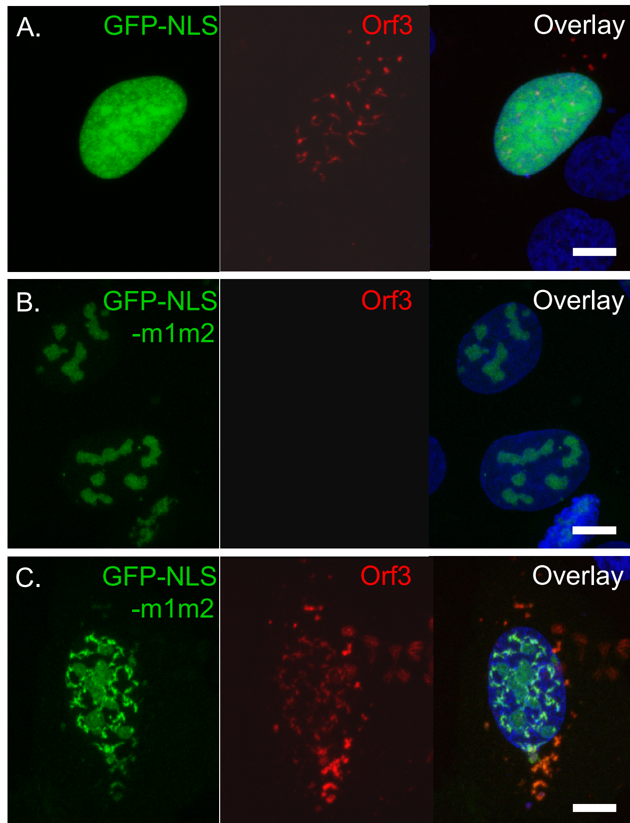

Figure 6

A.

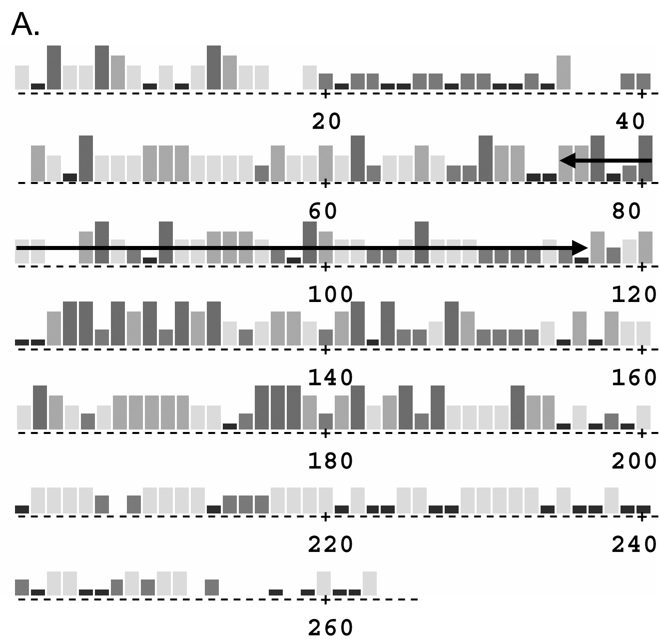

B.

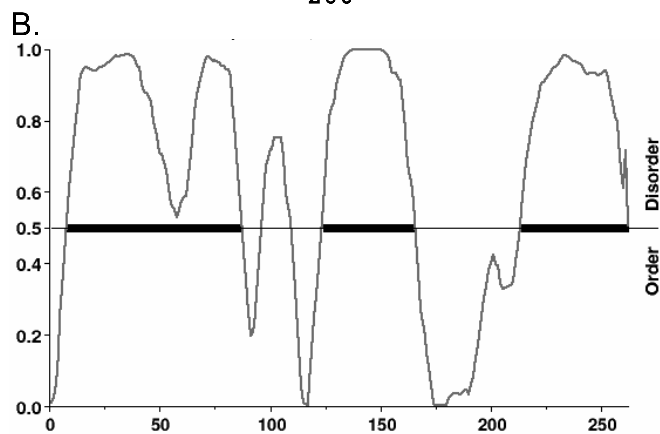

C.

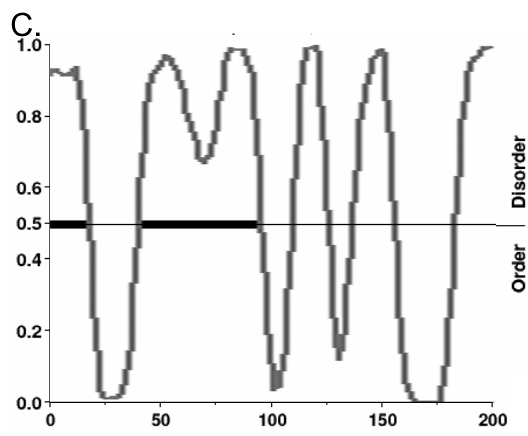

<u>Figure 7</u>

```
Rad50 (1312aa):   901 LYREI-KDAK-EQVSPLETTLEK 921
                      |||.  :. :  :  .|:. |::
PMLII:  HQERPAVHRGIRYLLYRAQ-RAIRLRHALRLHPQLHRAPIR
                     |||. :  : |||| ||
TIF1α (1050aa):  375 LLYSKRLITYRLRHLLR 391

                     ||:.       :|::||
TIF1β (835aa):   361 LLLSKKLIYFQLHRALK 377

                     |||:
SV40 large T:    170 LLYK 173   (708aa)

                        ||: :.: ||::
Ad5 L4 100K:        189 RAD-KQLALRQG 199 (807aa)
```